

New approach for solving electrocardiography imaging inverse problem with missing data on the body surface

Mohammed Addouche, Nadra Bouarroudj, Jacques Henry, Fadhel Jday, Nejib Zemzemi

► **To cite this version:**

Mohammed Addouche, Nadra Bouarroudj, Jacques Henry, Fadhel Jday, Nejib Zemzemi. New approach for solving electrocardiography imaging inverse problem with missing data on the body surface. Tendances des Applications Mathématiques en Tunisie, Algérie, Maroc 10-13 mai 2017, May 2017, Hammamet, Tunisia. hal-01567821

HAL Id: hal-01567821

<https://hal.inria.fr/hal-01567821>

Submitted on 24 Jul 2017

HAL is a multi-disciplinary open access archive for the deposit and dissemination of scientific research documents, whether they are published or not. The documents may come from teaching and research institutions in France or abroad, or from public or private research centers.

L'archive ouverte pluridisciplinaire **HAL**, est destinée au dépôt et à la diffusion de documents scientifiques de niveau recherche, publiés ou non, émanant des établissements d'enseignement et de recherche français ou étrangers, des laboratoires publics ou privés.

1. Introduction

Electrocardiographic imaging (ECGI) is a new technology that allows to non-invasively reconstruct the electretical activity of the heart from measurements on the body surface and geometrical informations of the torso. This clinical tool is used by cardiologists in order to localize some arrhythmogenic substrates, of particular concern are atrial and ventricular fibrillations. The current clinical tool consists of a vest containing 252 electrodes that are used to measure the electrical potential at the body surface and a software used to calculate the electrical potential on the heart surface. These electrodes are distributed on the body surface. The mathematical method used behind the tool the is Method of Fundamental Solutions (MFS) [11]. However, the 252 electrodes are not equally distributed on the torso surface and some regions are more covered than others. Moreover, in the clinical practice some electrodes are not considered in the inverse problem : Sometimes because they are not in contact with the patient skin and sometimes because of the high noise registered on some electrodes. This means that there are some regions where we know the potential and others where we don't have any information about the electrical potential. But in both cases, we know that the we have a zero flux boundary conditions in the whole body surface. In different studies [10, 7, 8], authors reconstruct these missing BSPs by interpolating them from the well measured signals.

In all works cited above and in most of the works that have been used in the literature for solving the ECGI inverse problem, the mathematical problem was formulated using a transfer matrix approach. This approach has been first introduced in [4]. The transfer matrix was later computed using different approaches like boundary elements, finite elements or MFS. Recent works [9, 12, 6] presented novel approches based on the recent advances on the boundary values inverse problem techniques. These works use an energy based cost function. The theoretical study of these methods has been reported in [2, 3, 1]. In this work we use the method of boundary value factorization introduced for solving data completion in [1]. It has been used for solving the ECGI problem in [6]. Our goal in this work is to introduce a new mathematical formulation that takes into account the missing data on the body surface without using interpolation methods. The missing BSPs would be part of the control problem.

2. Methods

2.1. Continuous Problem and Factorization Method

For the sake of simplicity and clarity, the problem is formulated on a cylindrical domain in all the paper. The cylindrical geometry and the Laplace operator make the presentation of the factorization method easy, but the method can be generalized to regular non-cylindrical domains and to more general self adjoint second-order elliptic operators. The generalization for a three dimensional domains could be done following. Let's consider the cylindrical domain Ω in \mathbb{R}^n . The domain $\Omega =]0, a[\times \theta$, where θ is a bounded domain in \mathbb{R}^{n-1} . The length of the cylinder a is a strictly positive real number. We denote by $\partial\Omega$ the boundary of the cylinder : $\partial\Omega = \Gamma_0 \cup \Gamma_a \cup \Sigma$, where $\Sigma =]0, a[\times \partial\theta$ is the lateral boundary of Ω , $\Gamma_0 = \Gamma_0^m \cup \Gamma_0^I = \{0\} \times \theta$ and $\Gamma_a = \{a\} \times \theta$ be the faces. The face θ , could be partitioned as follows $\theta = \theta^m \cup \theta^I$, so that $\{0\} \times \theta^m = \Gamma_0^m$ and $\{0\} \times \theta^I = \Gamma_0^I$. We suppose that Γ_0 is an accessible boundary, which means that we can measure the electrical potential on it. On the other hand Γ_a is inaccessible boun-

dary, which means that we cannot make any measurements on it. For the reasons that we cited previously, the boundary Γ_0^m is the part of Γ_0 where we have measurements of the potentials and in Γ_0^I we don't have electrical potential measurements.

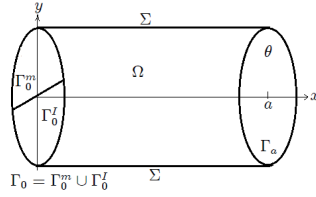


Figure 1 – Schematic representation of the cylindrical domain used in the study.

We also denote by $x \in \mathbb{R}$ the coordinate along the axis of the cylinder and by $y \in \mathbb{R}^{n-1}$ the coordinates in the section, perpendicular to the axis. The schematic representation of the domain Ω and all its boundaries is represented in Figure 1.

2.2. Optimal control problem

In this paper, we consider the following Continuous problem :

$$(p_0) \begin{cases} -\Delta u = 0 & \text{in } \Omega, \\ u = 0 & \text{on } \Sigma, \\ \nabla u \cdot n = 0 & \text{on } \Gamma_0, \\ u = T & \text{on } \Gamma_0^m. \end{cases} .$$

The boundary Γ_0^m is the measured portion of the surface of Γ_0 i.e the part of Γ_0 where we have both Dirichlet ($u = T$) and Neumann ($\nabla u \cdot n = 0$) boundary conditions. The boundary Γ_0^I is the unmeasured part of the surface Γ_0 i.e. it is the part of Γ_0 where we only know that we have a Neumann boundary condition ($\nabla u \cdot n = 0$). The data completion problem (p_0) is converted to an optimal control problem following the approach used in [2, 1, 6]. The difference is that now it includes three states instead of two. Each of them represents a boundary conditions on the accessible but incomplete boundary Γ_0^I and the inaccessible boundary Γ_a . For every triplet $(\eta, \tau, \tau') \in \left(H_{00}^{\frac{1}{2}}(\Gamma_a)\right)' \times H_{00}^{\frac{1}{2}}(\Gamma_a) \times H^{\frac{1}{2}}(\Gamma_0^I)$, we define the triplet of states (u_1, u_2, u_3) as follows

$$\begin{cases} -\Delta u_1 = 0 & \text{in } \Omega, \\ u_1 = 0 & \text{on } \Sigma, \\ u_1 = T & \text{on } \Gamma_0^m, \\ u_1 = 0 & \text{on } \Gamma_0^I, \\ \nabla u_1 \cdot n = \eta & \text{on } \Gamma_a. \end{cases} , \quad \begin{cases} -\Delta u_2 = 0 & \text{in } \Omega, \\ u_2 = 0 & \text{on } \Sigma, \\ \nabla u_2 \cdot n = 0 & \text{on } \Gamma_0, \\ u_2 = \tau & \text{on } \Gamma_a. \end{cases} , \quad \begin{cases} -\Delta u_3 = 0 & \text{in } \Omega, \\ u_3 = 0 & \text{on } \Sigma, \\ u_3 = 0 & \text{on } \Gamma_0^m, \\ u_3 = \tau' & \text{on } \Gamma_0^I, \\ \nabla u_3 \cdot n = 0 & \text{on } \Gamma_a. \end{cases} ,$$

where η , τ and τ' are the controls variables. For a given $\epsilon > 0$, we define the following cost functionals depending on the controls variables : The first uses the L^2 norm in the regularization operator

$$J_\epsilon^1(\eta, \tau, \tau') = \int_{\Omega} |(\nabla u_1 + \nabla u_3) - \nabla u_2|^2 dx dy + \epsilon \left(\|\eta\|_{L^2(\Gamma_a)}^2 + \|\tau\|_{L^2(\Gamma_a)}^2 + \|\tau'\|_{L^2(\Gamma_0^I)}^2 \right), \quad (1)$$

and in the second cost functional, we use the norm in the space where each variable lives.

$$J_\epsilon^2(\eta, \tau, \tau') = \int_{\Omega} |(\nabla u_1 + \nabla u_3) - \nabla u_2|^2 dx dy + \epsilon \left(\|\eta\|_{H_{00}^{\frac{1}{2}}(\Gamma_a)}^2 + \|\tau\|_{H_{00}^{\frac{1}{2}}(\Gamma_a)}^2 + \|\tau'\|_{H^{\frac{1}{2}}(\Gamma_0^I)}^2 \right). \quad (2)$$

We make use of the factorization method which transforms the elliptic boundary value problem into parabolic ones. This approach allows to compute the Dirichlet-to-Neuman and Neumann-to-Dirichlet mappings on a sequence of surfaces flowing from the known to the unknown boundaries. It allows a direct evaluation of the missing boundary data for any new Cauchy data T without re-computation of the operators [1, 6]. In what follows we will study the effect of the size of the area that lacks data by comparing the computed solution to a known analytical solution. We consider the problem (p_0) for $(x, y) \in]0, a[\times]0, \pi[$. The Cauchy data is given by $u(x, y)|_{\Gamma_0^m} = u(0, y)|_{\Gamma_0^m} = T = \sin(y)$, and $\nabla u(x, y)|_{\Gamma_0} \cdot n = \nabla u(0, y)|_{\Gamma_0} \cdot n = 0$. One can then check that : the harmonic function $u(x, y) = \cosh(x) \sin(y)$ is the solution of the problem. We seek to rebuild the data on the surface Γ_a and Γ_0^I . Data to be completed on Γ_a are : $\varphi_{\text{theo}} = \nabla u(a, y) \cdot n = \cosh(a) \sin(y) - \sinh(a) \cos(y)$, $t_{\text{theo}} = u(a, y) = \cosh(a) \sin(y)$. The exact incomplete data on Γ_0^I is $t'_{\text{theo}} = u(0, y) = \sin(y)$. We make use the methods developed in [1, 6] in order to solve the optimal control problem by minimizing J_ϵ^1 and J_ϵ^2 .

3. Results

In this section we present result of a numerical experiment to illustrate the effect of the size of the boundary where we measure the electrical potential $\% \Gamma_0^m$. We compare the exacts solution t_{theo} and t'_{theo} with the numerical solution t_{num} and t'_{num} . Let err_{regu1} and err_{regu2} be respectively the relative errors with respect to the first and the second regularizations. The error is computed at both the incomplete domains Γ_0^I and Γ_a . For this computation we took $\epsilon = 10^{-8}$ and $a = 2\pi$. Table 1 : Comparison of Integral regularization and norm regularization for the data completion problem with incomplete data. In Table 1, we provide err_{regu1} (respectively, err_{regu2}) the error between the exact solution and the solution obtained using the cost function J_ϵ^1 (respectively, J_ϵ^2), for various size of Γ_0^m . Without noise, we see that when the size of the measuring domain Γ_0^m is larger than 40% of the full accessible domain Γ_0 , the relative error is less than 1%. Whereas, when Γ_0^m is less than 10% of Γ_0 the relative error is higher than 10%. Figure2 shows the reconstructed potential at Γ_a when Γ_0^m covers 70% (left) and 12% (right)

$\% \Gamma_0^m$	90%	60%	40%	20%	10%	5%
err_{regu1}	$5,58.10^{-3}$	$6,76.10^{-3}$	$1,19.10^{-2}$	$3,79.10^{-2}$	$1,25.10^{-1}$	$2,7.10^{-1}$
err_{regu2}	$5,58.10^{-3}$	$6,84.10^{-3}$	$1,23.10^{-2}$	$3,83.10^{-2}$	$1,25.10^{-1}$	$2,7.10^{-1}$

Tableau 1 – Relative error between the exact solution and the solution obtained using the cost function J_ϵ^1 and J_ϵ^2 , for various size of Γ_0^m without noise.

Here, we also study the stability of the data completion problem to noise on the Dirichlet data. Let $err_{\text{regu1}}^\delta$ and $err_{\text{regu2}}^\delta$ the relative error when $\delta = 30\%$ is the added noise. The level of the noise is 30%. We see that the relative error of the solution si less than 5% when the size of Γ_0^m covers more than 80% of Γ_0 . The error is higher than 10% when the size of Γ_0^m covers less than 60% of Γ_0 . The error becomes too high when Γ_0^m covers less

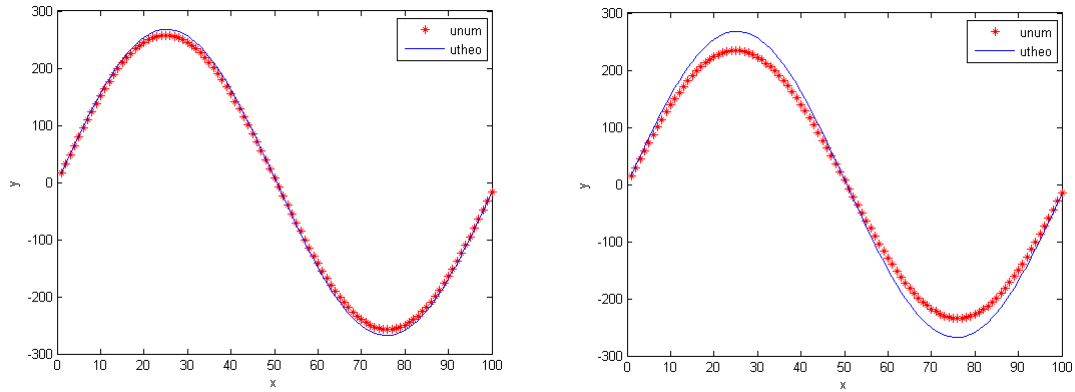


Figure 2 – Comparison between the exact (blue continuous ligne) and the computed (red stars) solutions. The area of Γ_0^m covers 20% (left) and 10% (right) than 20 of the accessible boundary as shown in Table 2. Figure3 shows the reconstructed potential at Γ_a when Γ_0^m covers 20% (left) and 10% (right)

$\% \Gamma_0^m$	90%	80%	70%	60%	20 %	15 %	12 %
err_{regu1}^δ	$2,16.10^{-2}$	$4,67.10^{-2}$	$6,87.10^{-2}$	$1,01.10^{-1}$	$3,23.10^{-1}$	$5,22.10^{-1}$	1.27
err_{regu2}^δ	$2,22.10^{-2}$	$4,88.10^{-2}$	$7,22.10^{-2}$	$1,08.10^{-1}$	$3,26.10^{-1}$	$5,24.10^{-1}$	1.28

Tableau 2 – Relative error between the exact solution and the solution obtained using the cost function $J_\epsilon^1(err_{regu1}^\delta)$ and $J_\epsilon^2(err_{regu2}^\delta)$, for various size of Γ_0^m with 30 of noise on the measured data.

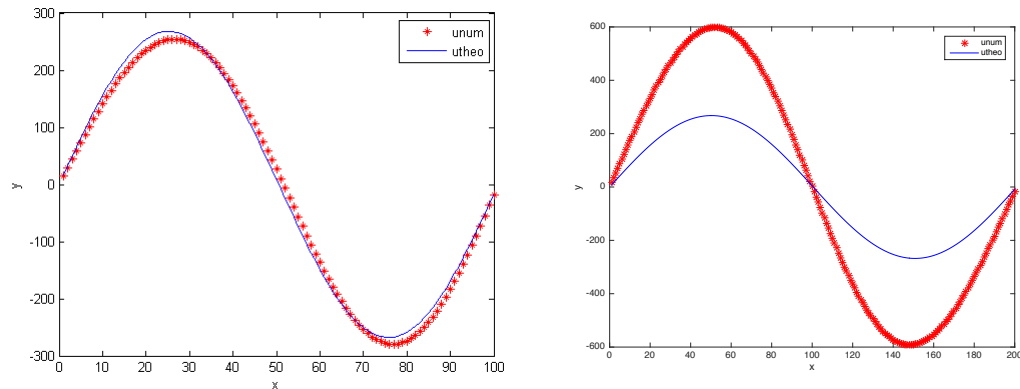


Figure 3 – Comparison between the exact (blue continuous ligne) and the computed (red stars) solutions when adding 30% of noise. The area of Γ_0^m covers 70% (left) and 12% (right) of the boundary Γ_0 .

4. Conclusion

In this paper, we presented a method to solve a data completion problem where the Cauchy data is measured on part of the accessible boundary. We used a method based on the factorization of elliptic boundary value problems. We numerically tested this method on a 2D rectangular domain. Without noise, results show that when the size of the measuring domain Γ_0^m is larger than 40% of the full accessible domain, the relative error is less than 1%. When Γ_0^m is less than 10% of Γ_0 the relative error is higher than 10%. Whereas, when the level of the noise is 30%, we found that the relative error of the solution is less than 5% when the size of Γ_0^m covers more than 80% of Γ_0 . The error is higher than 10% when the size of Γ_0^m covers less than 60% of Γ_0 . In future work, we aim to extend this study in 3D domain and theoretically study the effect of the size of the measuring domain.

Références

- [1] Amel Ben Abda, Jacques Henry, and Fadhel Jday. Boundary data completion : the method of boundary value problem factorization. *Inverse Problems*, 27(5) :055014, 2011.
- [2] Stephane Andrieux, Amel Ben Abda, and Thouraya Nouri Baranger. Data completion via an energy error functional. *Comptes Rendus Mécanique*, 333(2) :171–177, 2005.
- [3] Mejdî Azaïez, Faker Ben Belgacem, and Henda El Fekih. On cauchy’s problem : li. completion, regularization and approximation. *Inverse problems*, 22(4) :1307, 2006.
- [4] Roger C Barr, Maynard Ramsey III, and Madison S Spach. Relating epicardial to body surface potential distributions by means of transfer coefficients based on geometry measurements. *Biomedical Engineering, IEEE Transactions on*, pages 1–11, 1977.
- [5] Laura Bear, Mark Potse, Josselin Duchateau, Nejib Zemzemi, Yves Coudière, and Rémi Dubois. Accuracy of lead removal vs linear interpolation in non-invasive electrocardiographic imaging (ecgi). In *Computing in Cardiology Conference (CinC), 2015*. IEEE, 2014.
- [6] Julien Bouyssier, Nejib Zemzemi, and Jacques Henry. Inverse problem in electrocardiography via factorization method of boundary problems : how reconstruct epicardial potential maps from measurements of the torso ? In *International Symposium on Biomedical Imaging (ISBI), 2015*. IEEE, 2015.
- [7] John E Burnes, David C Kaelber, Bruno Taccardi, Robert L Lux, Philip R Ershler, and Yoram Rudy. A field-compatible method for interpolating biopotentials. *Annals of biomedical engineering*, 26(1) :37–47, 1998.
- [8] Alireza Ghodrati, Dana H Brooks, and Robert S MacLeod. Methods of solving reduced lead systems for inverse electrocardiography. *Biomedical Engineering, IEEE Transactions on*, 54(2) :339–343, 2007.
- [9] Nejla Hariga-Tlatli, TN Baranger, and Jocelyne Erhel. Misfit functional for recovering data in 2d electrocardiography problems. *Engineering Analysis with Boundary Elements*, 34(5) :492–500, 2010.

- [10] Thom F Oostendorp, Adriaan van Oosterom, and Geertjan Huiskamp. Interpolation on a triangulated 3d surface. *Journal of Computational Physics*, 80(2) :331–343, 1989.
- [11] Yong Wang and Yoram Rudy. Application of the method of fundamental solutions to potential-based inverse electrocardiography. *Annals of biomedical engineering*, 34(8) :1272–1288, 2006.
- [12] Nejib Zenzemi. A steklov-poincaré variational formulation of the inverse problem in cardiac electrophysiology. In *CinC-Computing in Cardiology Conference*, page 193. IEEE, 2013.